Eur. Phys. J. E **32**, 319–326 (2010)
DOI 10.1140/epje/i2010-10615-2

THE EUROPEAN PHYSICAL JOURNAL E

Regular Article

Nonlinearities in tilt and layer displacements of planar lipid bilayers

R. De Vita[1,a] and I.W. Stewart[2]

[1] Engineering Science and Mechanics Department, Virginia Tech, Blacksburg, VA, USA
[2] Department of Mathematics and Statistics, University of Strathclyde, Glasgow, UK

Received 12 September 2009 and Received in final form 24 February 2010
Published online: 8 July 2010 –

Abstract. A novel continuum model is proposed to describe the deformations of a planar lipid bilayer suspended across a circular pore. The model is derived within a new theoretical framework for smectic A liquid crystals in which the usual director **n**, which defines the average orientation of the molecules, is not constrained to be normal to the layers. The free energy is defined by considering the elastic splay of the director, the bending and compression of the lipid bilayer, the cost of tilting the director with respect to the layer normal, the surface tension, and the weak anchoring of the director. Variational methods are used to derive the equilibrium equations and boundary conditions. The resulting boundary value problem is then solved numerically to compute the fully nonlinear displacement of the layers and tilt of the lipid molecules. A parametric study shows that an increase in surface tension produces a decrease in the deformation of the lipid bilayers while an opposite effect is obtained when increasing the anchoring strength.

1 Introduction

Lipid bilayers constitute the base component of the cell membrane. Due to their important role in cell biology, lipid bilayers in various assemblies have been used in the development of many bioinspired systems such as, for example, drug delivery carriers [1,2], photovoltaic cells [3,4], and biosensors [5–7]. Planar lipid bilayers have been successfully employed as platforms for biosensors. The use of these sensors has been, however, limited thus far to laboratory environment since lipid bilayers are not stable and robust enough to resist air exposure and contamination, thermal and mechanical stresses during their transport, storage, and use in real-world enviroment [8].

Planar lipid bilayers for biosensors are usually suspended over single pores of micrometer and nanometer diameter or over solid substrates with multiple pores. Their lifetime and mechanical stability depends on the nature of the substrate [9]. The solvent used together with the lipid to form planar lipid bilayers remains trapped on the border region of the substrate forming the so-called annulus region, or Plateau-Gibbs border, which also affects the stability of these lipid structures [10,11]. Thus, efforts to improve the stability of planar lipid bilayers must be directed on understanding their interactions with the solvent and supporting substrates.

There has been a great deal of research on modeling the physical properties of lipid bilayers by employing molecular dynamics [12–15], coarse-grained models [16,17] and continuum models [18–20]. Molecular dynamics simulations are very powerful tools to study the microstructure of lipid bilayers, especially their interactions with different molecules and proteins. Due to current limitations in computing power, molecular dynamics can only be used to investigate phenomena that occur over length scales of tens of nanometers or time scales of tens of nanoseconds [16]. Coarse-grained models are formulated by glossing over atomic details and, thus, are less computationally expensive than molecular dynamics models.

Continuum models are preferred to simulate physical phenomena over long length and time scales that are relevant to many biological processes, experimental studies, and real-world applications involving lipid bilayers. One of the most successful continuum models for lipid bilayers is the *spontaneous curvature model* proposed by Helfrich [21]. This model has been derived from the Frank energy density for liquid crystals in which the normal to the membrane, **a**, coincides with the director, **n**, which defines the alignment of the constituent lipid molecules [22, 23]. It has been used by hundreds of researchers and, thus, citing all the great research that has followed from Helfrich's work is impossible. For example, Helfrich's model has been employed to study the deformations of lipid bilayers and their effects on channels and inclusions [24–27], interactions between inclusions in lipid bilayers [28], pressure effects [29].

As suggested by Helfrich [21], the tilt of the lipid molecules should also be taken into account when studying

[a] e-mail: devita@vt.edu

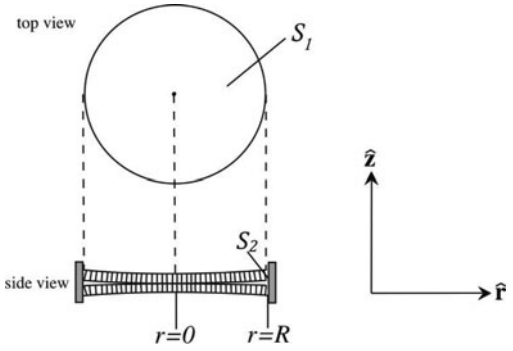

Fig. 1. Planar lipid bilayer suspended across a circular pore.

the mechanics of lipid bilayers. In the last decade, few investigators have incorporated the tilt of lipid molecules in continuum models for lipid bilayers [30–34]. While the continuum model proposed by May [32] is noteworthy since it accounts for different types of energetic contributions, it does not consider nonlinearities in the tilt and layer displacement.

In this paper, the tilt and layer deformations of a circular planar lipid bilayer anchored to a solid substrate are modeled by using a new theoretical framework for smectic A liquid crystals in which the average alignment of lipid molecules is not forced to be perpendicular to the layers [35]. Unlike the model presented by May [32], the tilt and displacement of the lipid bilayers are assumed to be fully nonlinear functions. The proposed model accounts for bending, compression, splay, and tension of the lipid bilayers and their anchoring to the substrate over which they are suspended. The model predictions agree qualitatively with experimental results that illustrate the distortions of planar lipid bilayer suspended over substrates with pores of micro-meter size. Specifically, the deformations of the bilayer and the tilting of the lipid molecules are pronounced in regions close to the boundary of the supporting substrates and increase with increasing anchoring strength and decreasing surface tension.

2 Model formulation

2.1 Theoretical framework

Consider a planar lipid bilayer suspended across a circular pore (as schematically shown in fig. 1 of [9]). The lipid bilayer can be assumed to have radial symmetry in the direction of the $\hat{\mathbf{r}}$-axis about the central $\hat{\mathbf{z}}$-axis as shown in fig. 1. Let $\mathcal{S}_1$ be the top or bottom circular surface of such a lipid bilayer with radius R, $\mathcal{S}_2$ its lateral surface, $\mathcal{V}$ its volume, and $2h$ its thickness. The planar lipid bilayer is assumed to be a smectic A liquid crystal in which the local preferred alignment of the molecules is defined by a unit vector $\mathbf{n}$, the so-called director. The molecules form a layer structure that can be described locally by a scalar function η or, equivalently, by a unit vector $\mathbf{a}$, which is normal to the layer structure. Hence, $\mathbf{a}$ is related to η by $\mathbf{a} = \nabla\eta/|\nabla\eta|$.

The following energy density, w_A, previously proposed for smectic A liquid crystals [35] and developed from the models discussed in [36–39], is used to model the lipid bilayer

$$w_A = \frac{1}{2}K_1^n(\nabla\cdot\mathbf{n})^2 + \frac{1}{2}K_1^a(\nabla\cdot\mathbf{a})^2 + \frac{1}{2}B_0(|\nabla\eta|-1)^2|\nabla\eta|^{-2} + \frac{1}{2}B_1\left\{1-(\mathbf{n}\cdot\mathbf{a})^2\right\}. \quad (1)$$

The energy density w_A in eq. (1) is invariant under the simultaneous changes in sign $\mathbf{n}\to-\mathbf{n}$ and $\mathbf{a}\to-\mathbf{a}$, which is equivalent to invariance under the simultaneous changes $\mathbf{n}\to-\mathbf{n}$ and $\nabla\eta\to-\nabla\eta$. The first term on the right-hand side of eq. (1) represents the elastic splay deformation of the director $\mathbf{n}$ while the second term describes the bending of the layer; both K_1^n and K_1^a are positive elastic constants. The third term is related to layer compression and is an extended version of that which is known from the classical descriptions of smectic A liquid crystals [40, 37,39]; B_0 is the positive layer compression constant. The fourth term accounts for the coupling between $\mathbf{n}$ and $\mathbf{a}$ with the positive constant B_1 having dimensions of energy per unit volume: in an equilibrium state this energy contribution is minimized when $\mathbf{n}$ and $\mathbf{a}$ are parallel. This term can also be written as $\frac{1}{2}B_1(\mathbf{n}\times\mathbf{a})^2$ as used in [38,39, 41], because $\mathbf{n}$ and $\mathbf{a}$ are unit vectors. The above model does not exclude the possibility that $\mathbf{n}$ and $\mathbf{a}$ may coincide at particular locations or regions.

For the planar lipid bilayer in the coordinate system shown in fig. 1, the layer normal $\mathbf{a}$ can be written as

$$\mathbf{a}(r) = -\sin\delta\,\hat{\mathbf{r}} + \cos\delta\,\hat{\mathbf{z}}, \quad (2)$$

where $\delta = \delta(r)$ is the angle formed by the layer normal with the $\hat{\mathbf{z}}$-axis and $0 \le r \le R$. The director $\mathbf{n}$ has the form

$$\mathbf{n}(r) = -\sin\theta\,\hat{\mathbf{r}} + \cos\theta\,\hat{\mathbf{z}}, \quad (3)$$

where $\theta = \theta(r)$ is the angle formed by the director with the $\hat{\mathbf{z}}$-axis and $0 \le r \le R$. Given eq. (2), the function $\eta = \eta(r,z)$, where $0 \le r \le R$ and $0 \le z \le h$, describing the layer structure can be found by solving the linear partial differential equation defined by

$$\mathbf{a} = \frac{\nabla\eta}{|\nabla\eta|}. \quad (4)$$

By using the method of characteristics (see Walker [42] for an example in smectics), the solution to eq. (4) is found to be

$$\eta(r,z) = c(z-u(r)), \quad (5)$$

where c is a dimensionless constant that reflects a change in the layer thickness measured relative to the initial layer thickness and $u(r)$ is the nonlinear displacement of the layer that is equal to

$$u(r) = \int_0^r \tan(\delta(t))\,\mathrm{d}t. \quad (6)$$

It must be emphasized that there is no assumption of small displacement in eq. (6). Indeed, the displacement u

is defined via η which is computed by solving the quasi-linear partial differential equation (4) and, hence, can be a fully nonlinear function. In a general mathematical description, η can be treated as an unknown function that must be determined in the process of finding solutions to the ensuing governing equations. A suitable choice of ansatz for η can vastly reduce the complexity of the mathematics and, quite naturally, it depends upon the anticipated geometry of the system being modeled. In the particular geometry being considered here, it is appropriate to select a form for η that is given by eq. (5), which is close to the one that describes a locally planar Cartesian geometry because the central part of the sample is predominantly close to a planar alignment of the lipid bilayer.

It then follows easily from eqs. (5) and (6) that

$$\nabla\eta = c\,(-\tan\delta\,\hat{\mathbf{r}} + \hat{\mathbf{z}})\,, \qquad |\nabla\eta| = c\sec\delta. \tag{7}$$

By using eqs. (2) and (3), one can easily show that

$$\nabla\cdot\mathbf{a} = -\frac{1}{r}\frac{\mathrm{d}}{\mathrm{d}r}(r\sin\delta), \qquad \nabla\cdot\mathbf{n} = -\frac{1}{r}\frac{\mathrm{d}}{\mathrm{d}r}(r\sin\theta), \tag{8}$$

$$\mathbf{n}\cdot\mathbf{a} = \sin\theta\sin\delta + \cos\theta\cos\delta = \cos(\theta-\delta), \tag{9}$$

$$1-(\mathbf{n}\cdot\mathbf{a})^2 = 1-\cos^2(\theta-\delta) = \sin^2(\theta-\delta). \tag{10}$$

Then, by using eqs. (7) to (10), the energy density in eq. (1) becomes

$$w_A = \frac{1}{2}K_1^n\frac{1}{r^2}\left[\frac{\mathrm{d}}{\mathrm{d}r}(r\sin\theta)\right]^2 + \frac{1}{2}K_1^a\frac{1}{r^2}\left[\frac{\mathrm{d}}{\mathrm{d}r}(r\sin\delta)\right]^2 + \frac{1}{2}B_0\left(1-\frac{\cos\delta}{c}\right)^2 + \frac{1}{2}B_1\sin^2(\theta-\delta). \tag{11}$$

The alignment of the lipid molecules at the surface $\mathcal{S}_2$ is assumed to be determined by a competition between the alignment of the molecules in the sample and their preferred alignment at the boundary. The director is thus assumed to be weakly anchored to the boundary and the flexibility of the director alignment at the surface is controlled by a finite anchoring strength that is linked to a surface energy term. In order to consider such weak anchoring of the director $\mathbf{n}$ on the surface $\mathcal{S}_2$, the following *weak anchoring energy density*, w_S, in the form of Rapini-Papoular [43,23] is employed:

$$w_S = \frac{1}{2}\tau_0(\mathbf{n}_R\times\mathbf{n}_p)^2 = \frac{1}{2}\tau_0[1-(\mathbf{n}_R\cdot\mathbf{n}_p)^2], \tag{12}$$

where $\mathbf{n}_R = \mathbf{n}(R)$ and $\mathbf{n}_p$ is the preferred alignment of the director at the boundary surface as indicated in fig. 2. The constant τ_0 which has the dimensions of surface tension ($\mathrm{J\,m^{-2}}$) measures the weak anchoring strength. The preferred alignment of the director at the boundary for the planar lipid bilayer shown in fig. 1 can be expressed as

$$\mathbf{n}_p = -\sin\theta_p\hat{\mathbf{r}} + \cos\theta_p\hat{\mathbf{z}}, \tag{13}$$

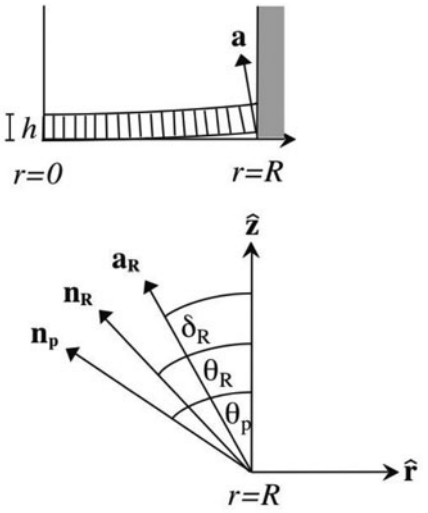

Fig. 2. Symmetry of a planar lipid bilayer suspended across a circular pore and coordinate system.

where θ_p is a fixed angle. Moreover,

$$\mathbf{n}_R = -\sin\theta_R\hat{\mathbf{r}} + \cos\theta_R\hat{\mathbf{z}}, \tag{14}$$

with $\theta_R = \theta(R)$. Hence, by calculations similar to those used in eqs. (9) and (10), one finds that $1-(\mathbf{n}_R\cdot\mathbf{n}_p)^2 = \sin^2(\theta_R-\theta_p)$ and therefore the weak anchoring energy density equation (12) takes the form

$$w_S = \frac{1}{2}\tau_0\sin^2(\theta_R-\theta_p). \tag{15}$$

There is still an unresolved controversy on the existence (and meaning) of surface tension in planar lipid bilayers [44,20]. In this study, the energetic contribution of surface tension, γ, for the planar lipid bilayer is assumed to be finite as previously considered by other investigators [45,25,26,20].

Finally, the total energy for the planar lipid bilayer considered here is

$$W = \int_{\mathcal{V}} w_A\mathrm{d}\mathcal{V} + \int_{\mathcal{S}_1} 2\gamma\mathrm{d}\mathcal{S}_1 + \int_{\mathcal{S}_2} w_S\mathrm{d}\mathcal{S}_2. \tag{16}$$

2.2 Equilibrium equations and boundary conditions

The equilibrium equations for the planar lipid bilayer can be determined by minimizing the total energy given by eq. (16) using variational methods [46]. Since $\theta = \theta(r)$ and $\delta = \delta(r)$, the minimization of eq. (16) over the planar lipid bilayer can be reduced via symmetry to the minimization of the same energy over a single planar lipid layer. Firstly, one needs to note that in eq. (16)

$$\mathrm{d}\mathcal{S}_1 = |\nabla\eta|\,r\,\mathrm{d}r\,\mathrm{d}\phi = \sec\delta\,r\,\mathrm{d}r\,\mathrm{d}\phi, \quad \mathrm{d}\mathcal{S}_2 = R\,\mathrm{d}z\,\mathrm{d}\phi,$$
$$\mathrm{d}\mathcal{V} = r\,\mathrm{d}r\,\mathrm{d}\phi\,\mathrm{d}z. \tag{17}$$

Then, the total energy of a single lipid layer can be written as

$$\begin{aligned} W &= \int_0^R \mathrm{d}r \int_0^{2\pi} \mathrm{d}\phi \int_0^h w_A r \,\mathrm{d}z \\ &\quad + \int_0^R \int_0^{2\pi} \gamma |\nabla \eta| r \,\mathrm{d}r \,\mathrm{d}\phi + \int_0^h \int_0^{2\pi} R w_S \,\mathrm{d}\phi \\ &= 2\pi h \int_0^R r w_A \,\mathrm{d}r + 2\pi \int_0^R \gamma |\nabla \eta| r \,\mathrm{d}r + 2\pi h \, R \, w_S \\ &= 2\pi \left\{ \int_0^R (h r w_A + c\gamma \, r \sec\delta) \,\mathrm{d}r + hR \, w_S \right\}. \end{aligned} \tag{18}$$

It is convenient to set $\bar{w}_A = r w_A$. A necessary condition for the total energy $W = W(r, \theta, \delta, \theta', \delta')$, where the prime symbol denotes the first derivative with respect to r, to have an extremum is that the Euler-Lagrange equations are satisfied [46], *i.e.*

$$\frac{\partial \bar{w}_A}{\partial \theta} - \frac{\mathrm{d}}{\mathrm{d}r}\left(\frac{\partial \bar{w}_A}{\partial \theta'}\right) = 0, \tag{19}$$

$$\frac{\partial \bar{w}_A}{\partial \delta} - \frac{\mathrm{d}}{\mathrm{d}r}\left(\frac{\partial \bar{w}_A}{\partial \delta'}\right) + \frac{c\gamma}{a} \sec\delta \tan\delta \, r = 0, \tag{20}$$

with boundary conditions

$$\frac{\partial \bar{w}_A}{\partial \theta'} + R \frac{\partial w_S}{\partial \theta} = 0, \quad \text{at } r = R, \tag{21}$$

$$\frac{\partial \bar{w}_A}{\partial \delta'} = 0, \quad \text{at } r = R, \tag{22}$$

$$\frac{\partial \bar{w}_A}{\partial \theta'} = 0, \quad \text{at } r = 0, \tag{23}$$

$$\frac{\partial \bar{w}_A}{\partial \delta'} = 0, \quad \text{at } r = 0. \tag{24}$$

The first of the above boundary conditions arises from the usual balance of couple condition [23] while the remaining boundary requirements are the usual natural boundary conditions that can be identified by a straightforward application of the theory of the first variation [46]. From the physical point of view, the system will compete between weak anchoring conditions and the internal alignment and it is this interplay that is reflected in the appropriate mathematical balance at equilibrium that leads to the balance of couples condition (*i.e.*, the natural boundary condition). By using eqs. (11) to (15), the equilibrium equations (19) and (20) can be rewritten as

$$\begin{aligned} &K_1^n \left[\cos^2\theta \,(r\theta'' + \theta') - \frac{1}{r} \sin\theta \cos\theta \,(1 + r^2\theta'^2)\right] \\ &\quad - B_1 r \sin(\theta - \delta)\cos(\theta - \delta) = 0, \end{aligned} \tag{25}$$

$$\begin{aligned} &K_1^a \left[\cos^2\delta \,(r\delta'' + \delta') - \frac{1}{r} \sin\delta \cos\delta \,(1 + r^2\delta'^2)\right] \\ &\quad - \frac{c\gamma}{h} \sec\delta \tan\delta \, r - B_0 r \sin\delta \left(1 - \frac{\cos\delta}{c}\right) \\ &\quad + B_1 r \sin(\theta - \delta)\cos(\theta - \delta) = 0, \end{aligned} \tag{26}$$

where the double prime symbol denotes the second derivative with respect to r.

Similarly, the boundary condition (21) can be rewritten as

$$2K_1^n \cos\theta_R \left[\frac{\sin\theta_R}{R} + \cos\theta_R \theta'(R)\right] + \tau_0 \sin(2(\theta_R - \theta_p)) = 0. \tag{27}$$

Substituting eq. (15) into the boundary condition (22) leads to

$$K_1^a \cos\delta_R \left[\frac{\sin\delta_R}{R} + \cos\delta_R \, \delta'(R)\right] = 0, \tag{28}$$

with $\delta_R = \delta(R)$. From eq. (28), it follows that

$$\delta'(R) = -\frac{1}{R} \tan\delta_R. \tag{29}$$

Again, for the form of weak anchoring energy (15), the boundary condition (23) becomes

$$K_1^n \cos\theta(0) \sin\theta(0) = 0. \tag{30}$$

Since $\theta(0) \neq \mp\frac{n\pi}{2}$ for $n = 1, 2, 3, \ldots$, the boundary condition (30) implies that

$$\theta(0) = 0. \tag{31}$$

Similarly, after substituting eq. (15) into the boundary condition (24), one obtains

$$\delta(0) = 0. \tag{32}$$

The previous equilibrium equations (25) and (26) and boundary conditions (27), (29), (31) and (32) can be non-dimensionalized by using the following set of constants:

$$\begin{aligned} &\lambda = \sqrt{\frac{K_1^n}{B_0}}, \quad B = \frac{B_1}{B_0}, \qquad \kappa = \frac{K_1^a}{K_1^n}, \quad \tau = \frac{\lambda \tau_0}{K_1^n}, \\ &\bar{r} = \frac{r}{h}, \qquad \alpha = \frac{c\gamma h}{K_1^n}, \quad \bar{R} = \frac{R}{h}, \quad m = \frac{h}{\lambda}, \end{aligned} \tag{33}$$

where λ is the typical length scale with dimensions of the layer [40]. The equilibrium equations (25) and (26) in non-dimensional forms are, respectively,

$$\begin{aligned} &\left[\cos^2\theta \,(\bar{r}\theta'' + \theta') - \frac{1}{\bar{r}} \sin\theta\cos\theta \,(1 + \bar{r}^2\theta'^2)\right] \\ &\quad - m^2 B \, \bar{r} \sin(\theta - \delta)\cos(\theta - \delta) = 0, \end{aligned} \tag{34}$$

$$\begin{aligned} &\kappa \left[\cos^2\delta \,(\bar{r}\delta'' + \delta') - \frac{1}{\bar{r}} \sin\delta\cos\delta \,(1 + \bar{r}^2\delta'^2)\right] \\ &- m^2 \bar{r} \sin\delta \left(1 - \frac{\cos\delta}{c}\right) + m^2 B \, \bar{r} \sin(\theta - \delta)\cos(\theta - \delta) \\ &- \alpha \, \bar{r} \sec\delta \tan\delta = 0, \end{aligned} \tag{35}$$

where the prime and double prime symbols now denote the first and second derivatives with respect to $\bar{r}$. The boundary conditions (27) and (28) at $\bar{r} = \bar{R}$ in non-dimensional

Table 1. Typical values of material parameters.

Parameter	Value	Unit	Reference
K_1^n, K_1^a	5×10^{-12}	N	[23]
B_0, B_1	8×10^5	$\mathrm{N\,m^{-2}}$	[53]
τ_0	10^{-3}	$\mathrm{N\,m^{-1}}$	[54]
γ	1.5×10^{-3}	$\mathrm{N\,m^{-1}}$	[53]
h	2.5×10^{-9}	m	[55]
R	10^{-4}	m	[9]
θ_p	$\pi/6$	rad	[47]

forms can be written as

$$2\cos\theta_R\left[\frac{\sin\theta_R}{\bar{R}} + \cos\theta_R\theta'(\bar{R})\right] + \tau\sin(2(\theta_R - \theta_p)) = 0, \tag{36}$$

$$\delta'(\bar{R}) = -\frac{1}{\bar{R}}\tan\delta_R, \tag{37}$$

while the boundary conditions (31) and (32) in non-dimensional form at $\bar{r} = 0$ are

$$\theta(0) = 0, \tag{38}$$
$$\delta(0) = 0. \tag{39}$$

The nonlinear displacement of the layer introduced in eq. (6) can be rewritten as

$$u(r) = h\hat{u}(\bar{r}), \tag{40}$$

where $\hat{u}(\bar{r})$ is the dimensionless displacement given by

$$\hat{u}(\bar{r}) = \int_0^{\bar{r}} \tan\delta\,\mathrm{d}\bar{r}. \tag{41}$$

Note that δ and θ that appear in the above dimensionless equations are computed over dimensionless $\bar{r}$.

3 Results

The above nonlinear system of equations and associated boundary conditions have been solved numerically using Maple 12 (Maple Inc., Waterloo, Canada). Typical values for the material parameters used for the numerical implementation are stated in table 1 and the corresponding values of the dimensionless parameters are $B = 1$, $\kappa = 1$, $\tau = 2.5 \times 10^{-2}$, $\alpha = 7.5 \times 10^{-1}$, $\bar{R} = 4 \times 10^4$, and $m = 1$. The constant c describing the expansion/compression of the lipid bilayers has been assumed to be 1 because it is anticipated to be close to unity, despite a lack of experimental information as to what its exact value may be. These base values have been used for computations except for any individual parameter that is allowed to vary in the graphs that are displayed below. The value of R has been chosen to be close to that used by Ries *et al.* [9]. In all cases, it is assumed that $m = 1$ because the length scale λ will always be approximately close to molecular dimensions [40]. The preferred alignment of the director at the boundary, θ_p, has been fixed at $\pi/6$; this value is actually determined by surface and interface properties and this particular value has been reported for smectic A samples [47].

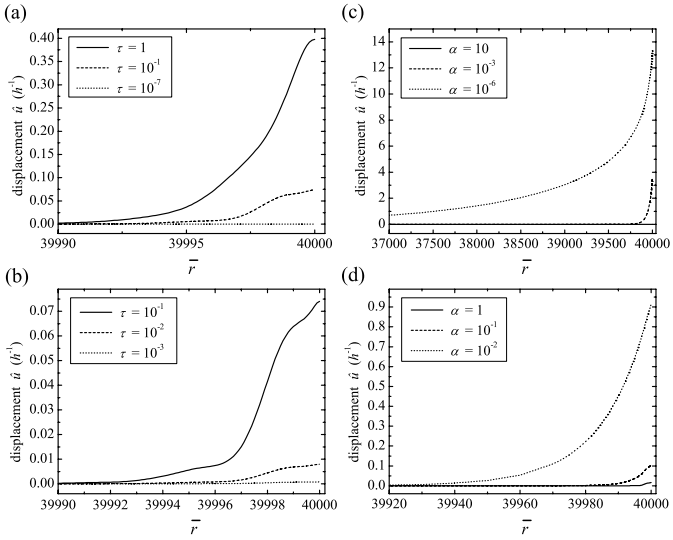

Fig. 3. The effects upon the dimensionless displacement $\hat{u}(\bar{r}) = u(r)/h$ due to varying the dimensionless anchoring strength τ are shown in (a) and (b) while those due to changing the surface tension α are shown in (c) and (d).

Figure 3 shows solutions for the layer displacement $\hat{u}(\bar{r})$ for selected values of the anchoring strength τ and surface tension α, the remaining material values being fixed at their typical base states. Figure 3(a) shows $\hat{u}(\bar{r})$ in units of the half-width, h, of the bilayer for low and high values of the anchoring strength ($\tau = 10^{-7}$, 10^{-1}, 1) while, for comparison, fig. 3(b) shows solutions for what are anticipated to be more realistically physical relevant values ($\tau = 10^{-3}$, 10^{-2}, 10^{-1}). For high anchoring magnitudes the layer displacement is greatest and at the boundary it is approximately 0.4 of the bilayer half-width h when $\tau = 1$; for values below $\tau = 10^{-2}$ the layer displacement appears to be less than 1% of the bilayer half-width. Moreover, it can be observed that, as the anchoring strength approaches zero, the *weak anchoring* boundary condition (27) reduces to the *no anchoring* boundary condition [23]. Without anchoring the lipid bilayer is free to distort at the boundary and presents many changes in curvature. Solutions for low and high values of the surface tension ($\alpha = 10^{-6}$, 10^{-3}, 10) are shown in fig. 3(c) with medium range values ($\alpha = 10^{-2}$, 10^{-1}, 1) displayed in fig. 3(d). It is evident that changing the surface tension has a more dramatic effect over a larger domain on the layer displacement than the corresponding changes in the anchoring strength. The medium value of $\alpha = 10^{-2}$ leads to a layer displacement that can be of the order of a bilayer half-width. Extremely small magnitudes of α can lead to excessively large layer displacements near the boundary, as seen in fig. 3(c). It is also noted that the

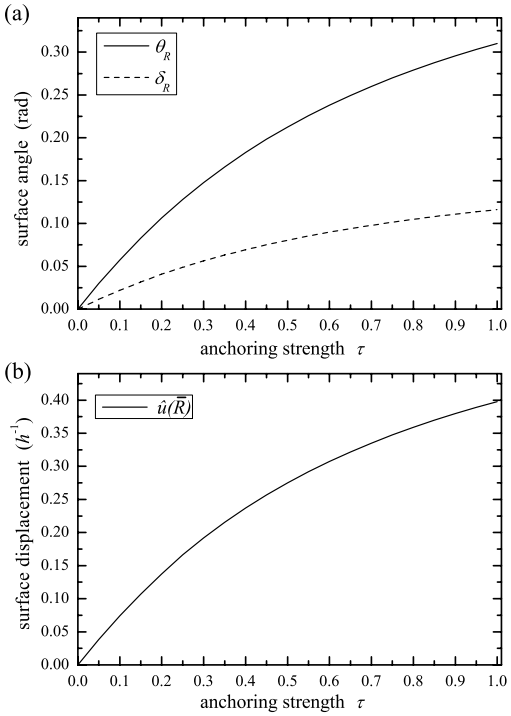

Fig. 4. The influence of the dimensionless anchoring strength $\tau = \lambda\tau_0/K_1^n$ upon (a) the boundary orientation angles, θ_R and δ_R, and (b) the layer displacement $\hat{u}(\bar{R})$ at the boundary surface.

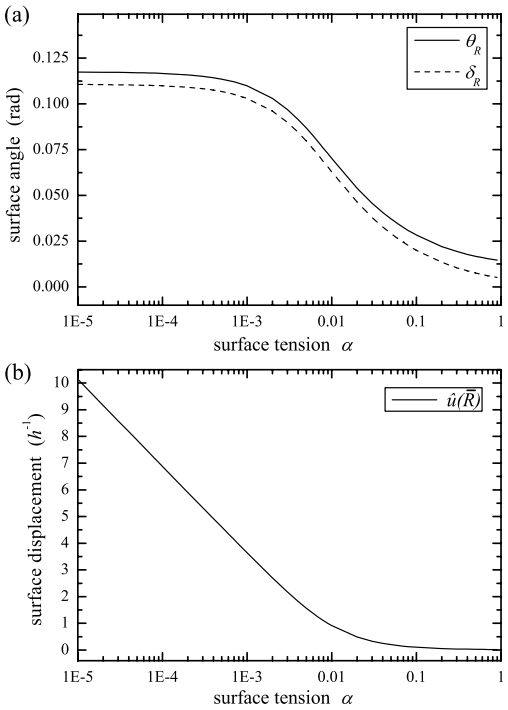

Fig. 5. The influence of the dimensionless surface tension $\alpha = c\gamma h/K_1^n$ upon (a) the boundary orientation angles, and (b) the layer displacement at the boundary surface. The horizontal axes are on a log scale to highlight the effects.

width of the boundary layer effect, the region over which there is greatest change in the plotted variables, is on a length scale of the order of ten bilayer half-widths as τ varies, whereas the boundary layer extends much more as α varies, as much as several thousand bilayer half-widths for extremely small magnitude surface tension.

Motivated by the numerical solutions presented in fig. 3, the key characteristics of the layer displacement and orientation angles for the director and layer normal are best indicated through their corresponding boundary surface values at $\bar{r} = \bar{R}$. Figure 4(a) shows the surface angles θ_R and δ_R for the director alignment and layer orientation at the boundary surface, respectively, and fig. 4(b) shows the corresponding layer displacement $\hat{u}(\bar{R})$ at the boundary. These quantities are seen to increase as the magnitude of τ increases. The results for surface tension, displayed on a horizontal log scale for clarity, are shown in fig. 5, where it is clear that θ_R, δ_R and $\hat{u}(\bar{R})$ are most sensitive to values of surface tension in the range $10^{-3} < \alpha < 10^{-1}$.

It is has been suggested on physical grounds [36] that B_1 should typically be of the order of B_0 or smaller. The results in fig. 6 happen to be in line with this suggestion since it is shown that the boundary surface values θ_R, δ_R and $\hat{u}(\bar{R})$ vary most when $B = B_1/B_0 \lesssim 1$. Figure 7 shows a similar effect when the anisotropy in the elastic constants $\kappa = K_1^a/K_1^n$ is smaller than unity, which indicates that a smaller layer bending modulus leads to a greater layer displacement and greater orientation angles at the boundary surface.

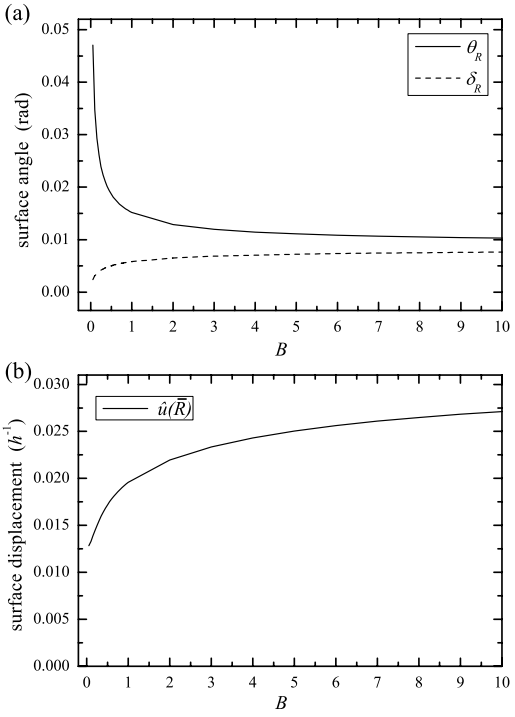

Fig. 6. The influence of varying $B = B_1/B_0$ upon (a) the boundary alignment angles, and (b) the layer displacement at the boundary surface.

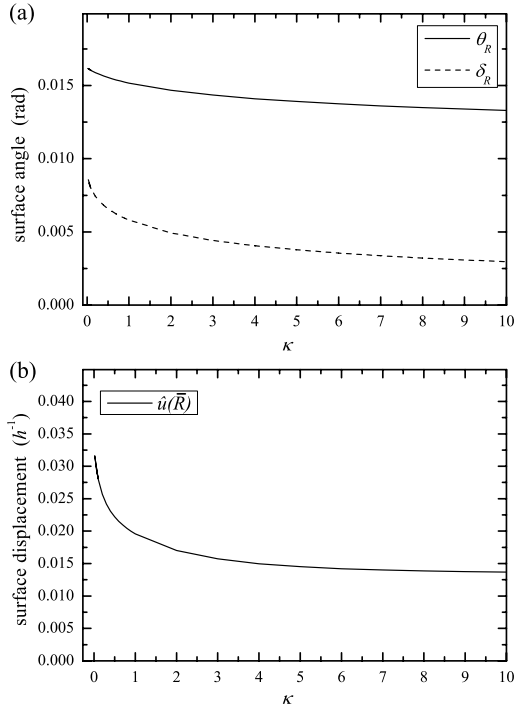

Fig. 7. The influence of varying the anisotropy in the elastic constants $\kappa = K_1^a/K_1^n$ upon (a) the boundary orientation angles, and (b) the layer displacement at the boundary surface.

4 Discussion

In this paper, layer and tilt deformations of circular planar lipid bilayers are studied in the context of the recent nonlinear theory for smectic A liquid crystals proposed by Stewart [35] in which the decoupling between the director and the normal to the smetic layers is taken into account. The novel features of this study are represented by the four key contributions to the energy density, w_A, stated in eq. (1) and the weak anchoring energy of the director mentioned in eq. (12). As discussed in sect. 2.1, the terms connected to K_1^n and K_1^a are directly related to the usual splay of the lipids and bending of the lamellar layer structure, respectively. The contribution due to compression is reflected in the B_0 term while the decoupling of the average alignment of the lipids away from the normal to the lipid bilayer is described by the B_1 contribution, a term first presented in [36] and exploited recently in the context of liquid crystals [38,39,48,41,49]. The introduction of weak anchoring in the context of lipid bilayers is novel and has also been applied recently [48] to a model of smectic A liquid crystals for the energy densities similar to the one discussed here. The coefficient τ_0 is a measure of the anchoring preference of the director to be parallel to a prescribed director surface alignment, directly related to the physical boundary conditions. It is well known that surface treatments in liquid crystals usually result in a preferred director alignment at the boundary that is not actually achieved because of competition with alignment preferences for the director away from the surface. It is this competition between alignments at the surface and away from it that creates the novel results that have been presented above in a nonlinear model formulation, especially in the description of the lipid bilayer displacement at the boundary, a feature that has been reported frequently in the literature [10].

The explicit expression for the layer displacement $u(r)$, given by eq. (6) and derived from an analysis of the layer function η, is a particularly prominent result: it allows the computation of the nonlinear layer displacement across the complete sample. This result, for a radial geometry, is analogous to that for planar geometries that was derived recently [49], a result that was anticipated by the numerical solutions of Anderson and Leslie [50] for planar aligned smectic liquid crystals.

The incorporation of surface tension in the total energy of lipid bilayers is still a subject of debate [51,44]. In this study, the surface tension is assumed to be finite as suggested by Brochard *et al.* [45] and can be interpreted as a chemical potential [20]. As expected, the results presented in figs. 3(c), (d) demonstrate that the deformation of the lipid bilayers drastically increases as the surface tension approaches zero becoming almost unrealistic.

The predictions of this theoretical study agree qualitatively with optical observations indicating the distortions of a lipid bilayer at its rim. The radius of the lipid bilayer for the boundary value problem considered here has been taken to be $100\,\mu$m in order to simulate the experimental setup presented by Ries *et al.* [9] where the lipid bilayer is formed over a single pore through a silicon substrate and imaged by using polarization-resolved second-harmonic generation microscopy (refer to fig. 1 of their manuscript). The numerical solutions capture the experimentally observed deformations in the proximity of the boundary but not their prolonged effect over almost half of the radius. Such effect is due to the presence of solvent trapped between the lipid bilayers and the supporting substrate. Indeed, recent work by Malmstadt *et al.* [52] indicate that the extension of the annulus region decreases significantly for solventless lipid bilayers (refer to fig. 3 of their manuscript). It is possible that the introduction of two interfacial tensions between the lipid bilayer and annulus and between the annulus and substrate need both to be considered to model the extended annulus region [10]. Because the values of these interfacial tensions and the values of all the parameters reported in table 1 are unknown for the specific lipids used in the experiments by Ries *et al.* [9] and by Malmstadt *et al.* [52], a quantitative and direct comparison between the proposed model and the experiments cannot be carried out.

Lipid bilayers are not static structures and undergo thermal fluctuations. Thus, future modeling efforts will focus on analyzing thermal fluctuations within the new dynamic theory for smectic A liquid crystals proposed by Stewart [35]. Based on previous findings [34], it is expected that the mathematical models will be able to describe short-wavelength fluctuations better than the Helfrich model since they account for the tilt of the lipid molecules with respect to the layer normal.

One aspect that may be of interest, which has not been considered, is the effect of van der Waals forces on the tilt

and layer deformations of lipid bilayers [56]. The angle formed by the lipid film in contact with the solvent, the so-called contact angle, and the thinning process of the film have been shown to strongly depend on the van der Waals interactions [57,58]. For this reason, future studies by the authors on the dynamics of lipid bilayers will incorporate these forces.

The authors would like to thank the Referees for their valuable comments which have greatly improved the quality of the manuscript.

References

1. G.V. Betangeri, S.A. Jenkins, D.L. Parsons, *Liposome Drug Delivery Systems* (Technomic Publishing Company, 1993).
2. U. Raviv, D.J. Needleman, Y. Li, H.P. Miller, L. Wilson, C.R. Safinya, Proc. Natl. Acad. Sci. U.S.A. **102**, 11167 (2005).
3. T.H. Tien, Nature **227**, 1232 (1970).
4. G. Steinberg-Yfrach, P.A. Liddell, S.C. Hung, A.L. Moore, D. Gust, T.A. Moore, J.L. Rigaud, E.N. Durantini, Nature **385**, 239 (1997).
5. T.H. Tien, A.L. Ottowa, Colloids Surf. A: Physicochem. Engin. Aspects **149**, 217 (1999).
6. I. Ivnitski, E. Wilkins, H.T. Tien, A. Ottova, Electrochem. Commun. **2**, 457 (2000).
7. K.M. Halverson, R.G. Panchal, T.L. Nguyen, R. Gussio, S.F. Little, M. Misakian, S. Bavari, J.J. Kasianowicz, J. Biol. Chem. **280**, 34056 (2005).
8. E. Reimhult, K. Katthik, Trends Biotechnol. **26**, 82 (2008).
9. R.S. Ries, H. Choi, R. Blunck, F. Bezanilla, J.R. Heath, J. Phys. Chem. B **108**, 16040 (2004).
10. S.H. White, Biophys. J. **12**, 432 (1972).
11. T.S.H. Snyder, K.G.E. Chiang, A.P. Tirio, J. Colloid Interface Sci. **67**, 31 (1978).
12. D.P. Tieleman, S.J. Marrink, H.J.C. Berendsen, BBA-Rev. Biomembranes **1331**, 235 (1997).
13. E. Jakobsson, Trends Biochem. Sci. **22**, 339 (1997).
14. L. Forrest, M.S.P. Sansom, Curr. Opin. Struct. Biol. **25**, 174 (2000).
15. S.E. Feller, Curr. Opin. Colloid Interface Sci. **5**, 217 (2000).
16. G. Brannigan, L.C.L. Lin, F.L.H. Brown, Eur. Biophys. J. **35**, 104 (2006).
17. M. Müller, K. Katsov, M. Schick, Phys. Rep. **434**, 113 (2006).
18. R. Lipowsky, U. Seifert, Mol. Cryst. Liq. Cryst. **202**, 17 (1991).
19. E. Evans, R. Skalak, *Mechanisms and Thermodyanmics of Biomembranes*, Vol. **64** (CRC, Boca Raton, FL, 1980).
20. F.L.H. Brown, Annu. Rev. Phys. Chem. **59**, 685 (2008).
21. W. Helfrich, Z. Naturforsch. **28**, 693 (1973).
22. F.C. Frank, Discuss. Faraday Soc. **25**, 19 (1958).
23. I.W. Stewart, *The Static and Dynamic Continuum Theory of Liquid Crystals* (Taylor & Francis, London and New York, 2004).
24. H.W. Huang, Biophys. J. **50**, 1061 (1986).
25. W. Helfrich, E. Jakobsson, Biophys. J. **57**, 1075 (1990).
26. C. Nielsen, M. Goulian, O.S. Anderson, Biophys. J. **74**, 1966 (1998).
27. P. Biscari, F. Bisi, R. Rosso, J. Math. Biol. **45**, 37 (2002).
28. H. Aranda-Espinoza, A. Berman, N. Dan, P. Pincus, S. Safran, Biophys. J. **71**, 648 (1996).
29. R. De Vita, I.W. Stewart, D.J. Leo, J. Phys. A: Math. Theor. **40**, 13179 (2007).
30. J.B. Fournier, Eur. Phys. J. B **11**, 261 (1999).
31. M. Hamm, M.M. Kozlov, Eur. Phys. J. E **3**, 323 (2000).
32. S. May, Eur. Biophys. J. **29**, 17 (2000).
33. S. May, Y. Kozlovsky, A. Ben-Shaul, M.M. Kozlov, Eur. Phys. J. E **14**, 299 (2004).
34. E.R. May, A. Narang, D.I. Kopelevich, Phys. Rev. E **76**, 21913 (2007).
35. I.W. Stewart, Continuum Mech. Thermodyn. **18**, 343 (2007).
36. R. Ribotta, G. Durand, J. Phys. (Paris) **38**, 179 (1977).
37. W. E, Arch. Rational Mech. Anal. **137**, 159 (1997).
38. G.K. Auernhammer, H.R. Brand, H. Pleiner, Rheol. Acta **39**, 215 (2000).
39. G.K. Auernhammer, H.R. Brand, H. Pleiner, Phys. Rev. E **66**, 061707 (2002).
40. P.G. de Gennes, J. Prost, *The Physics of Liquid Crystals*, second edition (Oxford Science Publications, 1993).
41. T. Soddemann, G.K. Auernhammer, H. Guo, B. Dünweg, K. Kremer, Eur. Phys. J. E **13**, 141 (2004).
42. A.J. Walker, J. Phys. A: Math. Theor. **41**, 385205 (2008).
43. A. Rapini, M. Papoular, J. Phys. Colloq. **30(C4)**, 54 (1969).
44. O. Farago, P. Pincus, Eur. Phys. J. E **11**, 399 (2003).
45. F. Brochard, P.G. de Gennes, P. Pfeuty, J. Phys. (Paris) **37**, 1099 (2006).
46. I.M. Gelfand, S.V. Fomin, *Calculus of Variations* (Dover, 2000).
47. S.J. Elston, Liq. Cryst. **16**, 151 (1994).
48. R. De Vita, I.W. Stewart, J. Phys.: Condens. Matter **20**, 335101 (2009).
49. I.W. Stewart, J. Phys. A: Math. Theor. **40**, 5297 (2007).
50. C. Anderson, F.M. Leslie, Mol. Cryst. Liq. Cryst. **330**, 609 (1999).
51. F. Jähnig, Biophys. J. **71**, 1348 (1996).
52. N. Malmstadt, T.J. Jeon, J.J. Schmidt, Adv. Mater. **20**, (2008).
53. S.B. Hladky, D.W.R. Gruen, Biophys. J. **38**, 251 (1982).
54. H. Yokoyama, H.A. Van Sprang, J. Appl. Phys. **57**, 4520 (1985).
55. R. Fettiplace, D.M. Andrews, D.A. Haydon, J. Membrane Biol. **5**, 277 (1971).
56. V.A. Parsegian, *Van der Waals forces: A Handbook for Biologists, Chemists, Engineers, and Physicists* (Cambridge University Press, 2006).
57. J.D. Requena, F. Billett, D.A. Haydon, Proc. R. Soc. London, Ser. A **347**, 141 (1975).
58. J. Requena, D.A. Haydon, Proc. R. Soc. London, Ser. A **347**, 161 (1975).